6-2005

Fluorescence-Dip Infrared Spectroscopy and Predissociation Dynamics of OH A (v=4) Radicals

Erika L. Derro

Ilana B. Pollack

Logan P. Dempsey

Margaret E. Greenslade
University of New Hampshire, Margaret.E.Greenslade@unh.edu

Yuxiu Lei

See next page for additional authors

Recommended Citation

E. L. Derro, I. B. Pollack, L. P. Dempsey, M. E. Greenslade, Y. Lei, D. Č. Radenović, M. I. Lester, "Fluorescence-Dip Infrared Spectroscopy and Predissociation Dynamics of OH A 2Σ+ (v=4) Radicals," J. Chem. Phys. 122, 24431 (2005).

Fluorescence-dip infrared spectroscopy and predissociation dynamics of OH A (v = 4) radicals

Erika L. Derro, Ilana B. Pollack, Logan P. Dempsey, Margaret E. Greenslade, Yuxiu Lei et al.

Citation: J. Chem. Phys. **122**, 244313 (2005); doi: 10.1063/1.1937387
View online: http://dx.doi.org/10.1063/1.1937387
View Table of Contents: http://jcp.aip.org/resource/1/JCPSA6/v122/i24
Published by the American Institute of Physics.

Fluorescence-dip infrared spectroscopy and predissociation dynamics of OH $A\,^2\Sigma^+$ ($v=4$) radicals

Erika L. Derro, Ilana B. Pollack, Logan P. Dempsey, Margaret E. Greenslade, Yuxiu Lei, Dragana Č. Radenović,[a] and Marsha I. Lester[b]
Department of Chemistry, University of Pennsylvania, Philadelphia, Pennsylvania 19104-6323

(Received 15 March 2005; accepted 27 April 2005; published online 28 June 2005)

Fluorescence-dip infrared spectroscopy, an UV-IR double-resonance technique, is employed to characterize the line positions, linewidths, and corresponding lifetimes of highly predissociative rovibrational levels of the excited $A\,^2\Sigma^+$ electronic state of the OH radical. Various lines of the $4 \leftarrow 2$ overtone transition in the excited $A\,^2\Sigma^+$ state are observed, from which the rotational, centrifugal distortion, and spin-rotation constants for the $A\,^2\Sigma^+$ ($v=4$) state are determined, along with the vibrational frequency for the overtone transition. Homogeneous linewidths of 0.23–0.31 cm^{-1} full width at half maximum are extracted from the line profiles, demonstrating that the $N=0$ to 7 rotational levels of the OH $A\,^2\Sigma^+$ ($v=4$) state undergo rapid predissociation with lifetimes of $\leqslant$23 ps. The experimental linewidths are in near quantitative agreement with first-principles theoretical predictions. © *2005 American Institute of Physics*.
[DOI: 10.1063/1.1937387]

I. INTRODUCTION

The hydroxyl radical (OH) has been the subject of many studies over the past several decades because of the key role that OH plays in atmospheric and combustion chemistry. In particular, the OH $A\,^2\Sigma^+$-$X\,^2\Pi$ band system has been well characterized using laser-induced fluorescence (LIF) spectroscopy since this is the primary method used for detection of OH in these environments. However, the utility of the A-X system is limited due to predissociation of the excited OH $A\,^2\Sigma^+$ electronic state, which results from curve crossings with three repulsive potentials, namely, $^4\Sigma^-$, $^2\Sigma^-$, and $^4\Pi$. Predissociation of the $A\,^2\Sigma^+$ state is induced by spin–orbit coupling in the intersection region(s), producing $O(^3P_J)+H(^2S)$ fragments.[1] Both theoretical and experimental works have been carried out to understand the nature of the curve crossings and predissociation dynamics of the OH $A\,^2\Sigma^+$ state. Theoretical studies have included predictions of predissociation rates, total (radiative plus radiationless) lifetimes, and $O(^3P_J)$ fine-structure distributions.[1–4]

Previous experimental studies have shown that high rotational levels in $v=0$ ($N\geqslant 24$) and $v=1$ ($N\geqslant 16$), as well as all N levels of $v=2$ and $v=3$ in the excited $A\,^2\Sigma^+$ electronic state, undergo predissociation.[5–10] In $v=2$, the rotationless level has a decay lifetime of ~150 ns,[7] which is about five times shorter than the 800-ns radiative lifetime.[11] Predissociation is 1000 times faster in $v=3$, with experimental measurements revealing decay lifetimes on the order of 0.2 ns for low-N levels.[8–10] In addition, the predissociation rate has been shown to increase with N for the $v=0$ to 3 vibrational levels of the OH $A\,^2\Sigma^+$ state.[8–10] For these vibrational levels, there is also good agreement between experiment and theory on the N-dependent predissociation rates, with predissociation resulting from interaction with a single repulsive ($^4\Sigma^-$) potential.[1]

Yet higher vibrational levels of the OH $A\,^2\Sigma^+$ state are expected to decay even more rapidly.[4] Prior experimental and theoretical studies of the $v=4$ state, the subject of the present study, indicate that predissociation occurs at least tenfold faster than in $v=3$. Theoretical predictions[1] and recent experimental measurements of $O(^3P_J)$ fine-structure distribution[12] also demonstrate that predissociation is due to interaction with all three dissociative potentials, $^4\Sigma^-$, $^2\Sigma^-$, and $^4\Pi$. The degree of interaction with a particular repulsive potential depends on the location of the $A\,^2\Sigma^+$ ($v=4,N$) rovibronic level relative to that curve crossing. At low N, predissociation is predicted to be predominantly due to interaction with the lowest repulsive potential ($^4\Sigma^-$), whereas the curve crossing with the highest repulsive potential ($^4\Pi$) is expected to dominate at higher N.[1] These multiple curve crossings could lead to an unusual N dependence in the predissociation rates for $v=4$.

Since nonradiative decay processes are much faster than the radiative decay for OH $A\,^2\Sigma^+$ ($v=4$), fluorescence emission is not easily detected, i.e., the quantum yield Φ_{fl} is ~0, making this state difficult to characterize experimentally. The OH $A\,^2\Sigma^+$ ($v=4$) state has been accessed previously in two studies, namely, through LIF excitation spectroscopy on the OH A-X (4,2) transition[13] and $B\,^2\Sigma^+ \rightarrow A\,^2\Sigma^+$ (1,4) fluorescence emission spectroscopy.[14] The LIF study obtained linewidths ranging from 0.65 to 1.0 cm^{-1} full width at half maximum (FWHM) for the OH $A\,^2\Sigma^+$ ($v=4,N=0-11$) rotational levels.[13] More recently, a theoretical study has predicted much narrower linewidths of ~0.3 cm^{-1} and corresponding lifetimes of $\leqslant$20 ps for OH $A\,^2\Sigma^+$ ($v=4,N=0-10$).[1,4] The considerable difference between the theoret-

[a]Permanent address: Department of Molecular and Laser Physics, University of Nijmegen, Toernooiveld 1, 6525 ED, Nijmegen, the Netherlands.
[b]Author to whom correspondence should be addressed; FAX: (215) 573-2112. Electronic mail: milester@sas.upenn.edu

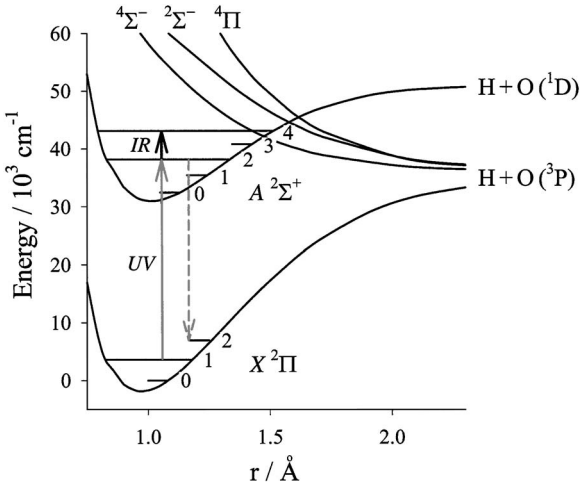

FIG. 1. Potential-energy diagram for the lowest bound states, $X\ ^2\Pi$ and $A\ ^2\Sigma^+$, and repulsive curves, $^2\Sigma^-$, $^4\Sigma^-$, and $^4\Pi$, of the OH radical adapted from Ref. 4. The repulsive potentials induce electronic predissociation of the $A\ ^2\Sigma^+$ state. Fluorescence-dip infrared (FDIR) spectra are obtained by promoting OH radicals to the $A\ ^2\Sigma^+$ ($v'=2$) state with the UV laser, and further exciting the OH radicals to the highly predissociative $A\ ^2\Sigma^+$ ($v=4$) state using an IR laser. Fluorescence emission (dashed line) is detected from the $A\ ^2\Sigma^+$ ($v'=2$) state exclusively.

ical predictions and previous experimental measurements of the linewidths for OH $A\ ^2\Sigma^+$ ($v=4,N$) levels suggested the need for further experimental investigation.

In the present work, an UV-IR double-resonance scheme is utilized to obtain the line positions and linewidths of several rovibronic levels in the OH $A\ ^2\Sigma^+$ ($v=4$) state. The UV and IR transitions are illustrated on a potential-energy diagram in Fig. 1. The UV laser promotes OH radicals from the $v''=1$ level of the ground $X\ ^2\Pi$ state to the $v'=2$ level of the electronically excited $A\ ^2\Sigma^+$ state. The IR laser further excites the OH radicals on an overtone transition to the $v=4$ level of the $A\ ^2\Sigma^+$ state. Fluorescence emission is detected from the $v'=2$ level of the $A\ ^2\Sigma^+$ state exclusively. When the IR laser is resonant with a $4\leftarrow 2$ overtone transition in the $A\ ^2\Sigma^+$ state, the population in $v'=2$ is depleted, resulting in a decrease in the fluorescence emission. A fluorescence-dip infrared (FDIR) spectrum is then obtained as the IR laser is scanned. The present study demonstrates the utility of the FDIR technique for obtaining detailed spectroscopic and dynamical information on highly predissociative levels of the OH radical in its excited $A\ ^2\Sigma^+$ state.

II. EXPERIMENT

Hydroxyl radicals are produced by photolysis of the vapor from 99.5 wt % HNO_3 (Aldrich) entrained in He carrier gas (35 psi) using 193-nm radiation from an ArF excimer laser (Lambda Physik, Complex 102 or LPX 105i). The gas mixture is photolyzed within a quartz capillary tube[15] attached to the exit flange of a solenoid pulsed valve assembly (General Valve, Series 9). The OH radicals are relaxed to some extent by collisions with He carrier gas as the mixture undergoes supersonic expansion in the vacuum chamber. The OH radicals are subsequently promoted to highly predissociative levels of the excited $A\ ^2\Sigma^+$ electronic state using a sequential UV-IR excitation scheme, which is described briefly in the Introduction and explained in more detail in the Results and Analysis section. The experimental section focuses on the laser setup and data-acquisition procedure.

Tunable UV radiation near 288 nm is generated by frequency doubling [potassium dihydrogen phosphate (KDP)] the output of a Nd:yttrium aluminum garnet (YAG) pumped dye laser (Continuum 7020 or Surelite II YAG with a ND 6000 dye laser, 7-ns pulse, 20-Hz repetition rate) operating with a Rhodamine 590/610 dye mix. Typically, 1–2 mJ/pulse of UV radiation ($\sim$0.15-cm^{-1} bandwidth) is passed into the vacuum chamber. The UV laser is calibrated using the well-known frequencies of OH A-X (2,1) lines.[11,16]

Tunable IR radiation in the vicinity of 2 μm is generated using two different optical parametric oscillator (OPO) systems. Both OPO systems are pumped by injection-seeded Nd:YAG lasers (Continuum Precision 8000, 7–8-ns pulse width, 10-Hz repetition rate). The IR transitions were initially identified with a 0.15-cm^{-1} bandwidth OPO (LaserVision) that delivers up to 10 mJ/pulse of IR radiation. This OPO operates with a 532-nm radiation to pump the potassium titanyl phosphate (KTP) oscillator and 1064-nm radiation to pump the potassium titanyl arsenate (KTA) amplifier stage. Linewidth measurements were then made using a single longitudinal mode OPO (Continuum Mirage 3000) with a narrow bandwidth (0.02 cm^{-1}) that generates up to 5 mJ/pulse of IR radiation. The 532-nm pumped master oscillator (MO) operates on a single longitudinal mode by active cavity length stabilization. The signal output of the KTP-based MO beam is amplified in a KTP nonresonant oscillator (NRO), which simultaneously produces the desired near-infrared idler beam.

The absolute and relative frequencies of each OPO are calibrated with each scan. Absolute frequency markers are established by recording a CO_2 photoacoustic spectrum and comparing the observed lines with well-documented transitions in the HITRAN database.[17] Relative frequency markers are generated by passing the signal output of the oscillator through an etalon [free spectral range (FSR) $\sim$0.20 or 0.34 cm^{-1}]. The relative frequency scale of each spectrum is determined by linear interpolation between adjacent fringes of the etalon trace to correct for nonlinearities introduced by mechanical imperfections in the motor and/or piezodriven stages of the OPO.[18,19] The absolute frequency of each line in the FDIR spectra is established by fitting the data to both photoacoustic and etalon traces simultaneously.

The UV and IR laser beams are counterpropagated into the vacuum apparatus, where they are spatially overlapped in the collision-free region of the supersonic expansion approximately 1.5 cm downstream from the exit of the quartz capillary tube. The UV beam is unfocused with a 5-mm diameter; the IR beam is attenuated and defocused as needed to reduce the power density inside the chamber. The OH LIF signal is collected using $f/1$ optics and detected with a photomultiplier tube (EMI 9813Q) positioned perpendicular to both the laser and supersonic expansion axes. A bandpass filter centered at 320±10 nm is used to block the scattered light arising from the UV laser, while still passing fluorescence in the OH A-X (2,2) spectral region. The fluorescence signal is preamplified, integrated over a 50–200-ns gate (de-

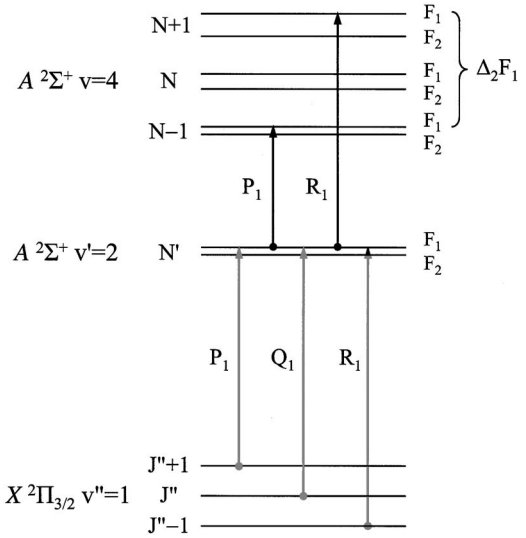

FIG. 2. Schematic energy-level diagram illustrating the UV-IR double-resonance scheme used to access individual rotational levels of the excited OH $A\ ^2\Sigma^+$ $(v=4,N)$ state. UV laser excitation on a P_1 line (see text) of the A-X (2, 1) transition prepares the $A\ ^2\Sigma^+$ $(v'=2,N',F_1)$ state. Subsequent excitation on a P_1 or R_1 line of the IR overtone transition promotes population to the $A\ ^2\Sigma^+$ $(v=4, N-1$ or $N+1, F_1)$ state; the energy difference Δ_2F_1 is used in the spectroscopic analysis. Only one Λ-doublet component of each ground-state level is depicted, and thus UV satellite lines $(\Delta J \neq \Delta N)$ are not shown. Note that the $N=0$ level of the $A\ ^2\Sigma^+$ state has only an F_1 spin component.

pending on the lifetime of the fluorescing state), and transferred to a laboratory computer for further analysis.

The lasers are synchronized such that the IR laser (10 Hz) is present for every other UV laser pulse (20 Hz). The UV laser pulse typically precedes the IR laser pulse by 20 ns. The "UV only" signal is subtracted from the "UV +IR" signal on alternating pulses to yield "fluorescence-normalized" FDIR spectra, with data stored as [(UV+IR) −UV].[20] This active base line subtraction procedure corrects for fluctuations in the UV-induced fluorescence signal. In addition, the "UV only" signal is retained on a separate data-acquisition channel. Typically, the fluorescence-normalized FDIR signal arising from 150 laser shots (75 IR+UV and 75 UV only) is collected and averaged for each data point.

III. RESULTS AND ANALYSIS

A sequential UV-IR double-resonance excitation technique is used to access individual rotational levels of the excited OH $A\ ^2\Sigma^+$ $(v=4)$ state, which is illustrated in Fig. 2. The UV transition is carefully selected to prepare a single rovibronic level of the excited OH $A\ ^2\Sigma^+$ $(v'=2,N')$ state (see below); the IR laser subsequently promotes the OH radicals to strongly predissociative rotational levels of the OH $A\ ^2\Sigma^+$ $(v=4)$ state. FDIR spectra of the $4\leftarrow2$ overtone transition in the excited OH $A\ ^2\Sigma^+$ electronic state are obtained by scanning the IR laser and detecting the resultant dips in the fluorescence emission from the $A\ ^2\Sigma^+$ $(v'=2)$ state. The transition frequencies and linewidths of various P- and R-branch lines of the overtone transition are measured. The homogeneous linewidths are then used to determine the predissociation lifetimes for the $N=0$ to 7 rotational levels (F_1 spin component) of the OH $A\ ^2\Sigma^+$ $(v=4)$ state. The standard spectroscopic notation for the OH $A\ ^2\Sigma^+$ state is used here,[16,21] as briefly summarized in Ref. 22.

TABLE I. Absolute frequency and linewidths for rovibrational transitions of the $4\leftarrow2$ overtone band in the excited OH $A\ ^2\Sigma^+$ electronic state. The corresponding lifetime of each OH $A\ ^2\Sigma^+$ $(v=4,N)$ level is derived from the experimental linewidth.

OH $A\ ^2\Sigma^+$ $(v=4,N)$	IR transition	Transition wave number (cm^{-1})[a]	Lorentzian linewidth (cm^{-1})[b]	Lifetime (ps)
0	$P_1(1)$	4948.46(8)	0.24(3)	22(3)
1	$P_1(2)$	4914.69(8)	0.23(5)	23(5)
2	$P_1(3)$	4876.90(8)	[c]	⋯
3	$P_1(4)$	4835.99(8)	[c]	⋯
4	$P_1(5)$	4791.73(8)	[c]	⋯
2	$R_1(1)$	5029.70(8)	0.29(3)	18(2)
3	$R_1(2)$	5049.34(8)	0.26(6)	21(5)
4	$R_1(3)$	5065.54(8)	0.27(5)	20(4)
5	$R_1(4)$	5077.90(8)	0.26(5)	21(4)
6	$R_1(5)$	5086.38(8)	0.30(6)	18(4)
7	$R_1(6)$	5091.01(8)	0.31(6)	17(3)

[a]Repeated measurements of the line positions have yielded an uncertainty (1σ) of 0.08 cm^{-1} as compared to the IR laser bandwidth of 0.15 cm^{-1}.
[b]The uncertainty in the linewidth reflects the standard deviation (1σ) from multiple determinations; an IR laser bandwidth of 0.02 cm^{-1} was utilized for linewidth measurements.
[c]Linewidths were not measured for these P_1 lines; instead, the stronger R_1 lines that accessed the same OH $A\ ^2\Sigma^+$ $(v=4,N)$ level were utilized.

Various OH A-X (2,1) lines can be used to prepare the intermediate OH $A\ ^2\Sigma^+$ $(v'=2,N')$ state, as shown in Fig. 2. The UV transitions originate from OH $X\ ^2\Pi_{3/2}$ $(v''=1,J'')$ levels that are populated upon photolysis of HNO_3, and rotationally relaxed to some extent in the He expansion.[23] In principle, it would seem most favorable to use R_1 or Q_1 lines for the UV transition since these transitions have stronger line strength factors than P_1 lines under saturated LIF conditions.[30] Also, the R_1 and Q_1 lines that prepare a given OH $A\ ^2\Sigma^+$ $(v'=2,N')$ state would originate from the more populated J'' and $J''-1$ rotational levels rather than the $J''+1$ level that is the origin of P_1 lines. However, both R_1 and Q_1 lines have nearby satellite lines $(\Delta J \neq \Delta N)$, particularly at low J'', which are not resolved from these main branch $(\Delta J = \Delta N)$ lines at the experimental UV linewidth. The main branch lines prepare the upper-F_1 spin component of the OH $A\ ^2\Sigma^+$ $(v'=2,N')$ state, while the weaker satellite lines prepare the lower-F_2 spin component. Since this is a double-resonance experiment, the satellite lines associated with UV transitions only become a problem if the subsequent IR overtone transitions originating from the F_1 and F_2 sublevels are also close in frequency. This is indeed the case at low N', where the P_1 and P_2 or R_1 and R_2 lines of the infrared overtone transition are expected to overlap one another. As a result, it was necessary to use P_1 lines for the OH A-X (2,1) transitions at low J'', since they do not have nearby satellite lines and therefore permit preparation of individual quantum levels of the OH $A\ ^2\Sigma^+$ $(v'=2,N',F_1)$ state.

A least-squares fit to a Voigt line profile is used to extract the central frequencies and Lorentzian linewidths of the individual dips in the FDIR spectra (Table I). The Gaussian

TABLE II. Spectroscopic constants (cm^{-1}) for OH $A\,^2\Sigma^+$ ($v=4$) derived from the $4\leftarrow2$ overtone band, and comparison with values from a merged fit and Dunham coefficients.

Parameter	Present work analyzed by combination differences	Present work fit by transition wave numbers	Coxon *et al.* merged fit[a]	Dunham coefficients[b]
$G(4)$	10 760.80(8)	10 760.9(1)	10 760.84[c]	10 760.859
ν_0	4 979.13(8)	4 979.2(1)	4 979.17[c]	4 979.087
B_4	13.50(3)	13.51(3)	13.517 2(22)	13.520 4
D_4	0.001 8(4)	0.002 1(3)	0.002 38(15)	...[d]
γ_4	0.2(3)	0.2(3)	0.178(10)	...[d]

[a]See Table III of Ref. 32.
[b]See Table I of Ref. 33.
[c]Derived from term values in Refs. 31 and 32.
[d]Relevant coefficients not reported in Ref. 33.

parameter of these fits is fixed at the laser bandwidth, 0.02 or 0.15 cm^{-1} FWHM, while the central frequency, Lorentzian linewidth, base line, and amplitude are variable parameters of the least-squares fit. For each fit, the base line is checked to make sure it returns to zero, while the amplitude is used to obtain the magnitude of the depletion. The central frequencies derived from three measurements of each line are averaged to obtain the reported line positions. In addition, six independent measurements of each P_1 or R_1 line in the FDIR spectrum are recorded, analyzed to extract their Lorentzian linewidths, and averaged to obtain the reported values. The Lorentzian linewidths are then used to obtain lifetimes for the predissociative levels.

The transition frequencies of the F_1 components of the $P_1(1)$-$P_1(5)$ and $R_1(1)$-$R_1(6)$ lines associated with the $4\leftarrow2$ overtone transition in the excited $A\,^2\Sigma^+$ electronic state are determined in this work. The rotational term values for the F_1 levels in a $^2\Sigma^+$ electronic state are defined according to the following standard expression:[21]

$$F_1(N) = B_v N(N+1) - D_v[N(N+1)]^2 + \frac{1}{2}\gamma_v N,$$

where B_v is the rotational constant, D_v is the centrifugal distortion constant, and γ_v is the spin-rotation coupling constant. The upper-state combination differences, i.e., the energy difference between P and R transition originating from a common N level, can be expressed as

$$\Delta_2 F_1(N) = (4B_v - 6D_v)\left(N+\frac{1}{2}\right) - 8D_v\left(N+\frac{1}{2}\right)^3 + \gamma_v.$$

From analysis of combination differences associated with five different N levels in a weighted least-squares fit, the spectroscopic constants are determined to be $B_4 = 13.50(3)$ cm^{-1}, $D_4 = 0.0018(4)$, and $\gamma_4 = 0.2(3)$ cm^{-1} (see Table II). The band origin ν_0 is found to be 4979.13(8) cm^{-1} based on the experimental $P_1(1)$ line position and previously reported spectroscopic data for OH $A\,^2\Sigma^+$ ($v'=2$).[31] The spectroscopic constants (ν_0, B_4, D_4, and γ_4) were also evaluated in a separate least-squares-fitting procedure that minimizes the squares of the residuals between the observed and calculated positions of these 11 lines, while holding the rotational constants for $v'=2$ at their literature values.[31] The two procedures yield nearly the same values for the spectroscopic constants (see Table II). The vibrationally averaged internuclear separation for OH $A\,^2\Sigma^+$ ($v=4$) is thus found to be 1.147(1) Å. Furthermore, the vibrational energy $G(4)$ is determined to be 10 760.80(8) cm^{-1} relative to $A\,^2\Sigma^+$ ($v=0, N=0$). Unfortunately, the spin-rotation constant, γ_4, previously estimated to be on the order of ~0.18 cm^{-1},[32] is not well determined from the present spectroscopic data.

The FDIR spectroscopy technique was initially tested for linewidth measurements using an IR overtone transition to access predissociative levels in the OH $A\,^2\Sigma^+$ ($v=3$) state that have been previously characterized.[8,9] For this experiment only, the UV laser excites a rovibronic transition in the OH $A\,^2\Sigma^+ - X^2\Pi(1,0)$ region; the IR laser subsequently excites OH on the $3\leftarrow1$ overtone transition in the $A\,^2\Sigma^+$ state. The overtone transition was found to be readily saturated by the unfocused output of the single-mode OPO. As a result, it was necessary to attenuate the IR power density by defocusing and/or using neutral density filters to obtain a homogeneous linewidth that reflects the true predissociative lifetime of the OH $A\,^2\Sigma^+$ ($v=3, N$) state. The power density was reduced sufficiently to obtain a Lorentzian linewidth of $\Gamma = 0.065$ cm^{-1} (FWHM) for the $P_1(10)$ line of the $3\leftarrow1$ overtone transition (see Fig. 3) as a test case. This homogenous linewidth observed for the transition terminating on the F_1 component of the OH $A\,^2\Sigma^+$ ($v=3, N=9$) state agrees well with the previously determined values of 0.06–0.07 cm^{-1},[8–10] verifying the applicability of the FDIR technique for linewidth measurements.

Linewidth measurements were then carried out for overtone transitions that access the $N=0$ to 7 levels of the OH $A\,^2\Sigma^+$ ($v=4$) state (F_1 spin component). The resultant line profiles are shown in Fig. 3 with central frequencies aligned on a relative wave-number scale and amplitudes scaled to a constant value. The Lorentzian linewidths extracted from the Voigt line profiles along with the IR transitions used to make these measurements are given in Table I. The Lorentzian linewidths range from 0.23 to 0.31 cm^{-1} and are significantly broader than that observed for OH $A\,^2\Sigma^+$ ($v=3, N=9$), indicating much faster predissociation rates for $v=4$. The corresponding lifetimes for OH $A\,^2\Sigma^+$ ($v=4, N=0$–7) are also tabulated in Table I.

The percentage depletion in FDIR spectra is evaluated according to

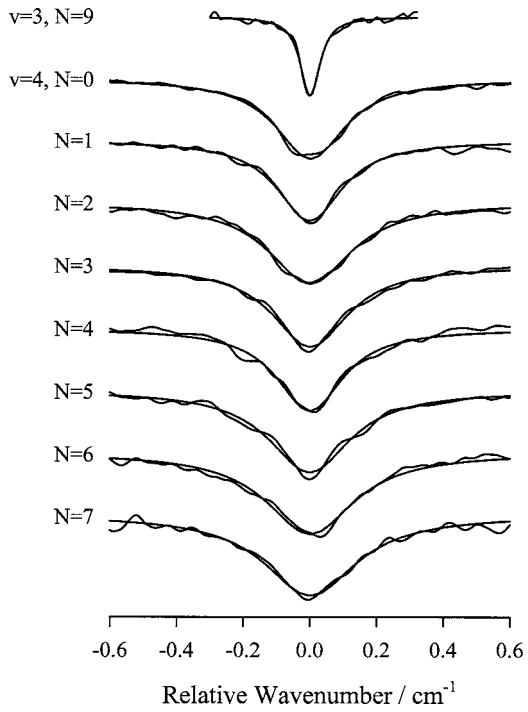

FIG. 3. Fluorescence-dip infrared (FDIR) spectra of rovibrational lines in the $3 \leftarrow 1$ and $4 \leftarrow 2$ overtone bands of the excited OH $A\ ^2\Sigma^+$ state plotted on a relative wave-number scale. Various P_1 and R_1 lines (Table I) are used to access the OH $A\ ^2\Sigma^+$ $v=3$, $N=9$ and $v=4$, $N=0-7$ levels. The line profiles are fit to a Voigt line shape (smooth curve through data) to extract the frequencies and Lorentzian linewidths of individual dips in the FDIR spectra.

$$\left| \frac{[\mathrm{UV}+\mathrm{IR}]-\mathrm{UV}}{\mathrm{UV}_{\mathrm{ave}}} \right| 100\ \%\ ,$$

where $\mathrm{UV}_{\mathrm{ave}}$ is the average signal level on the UV only channel during a dip measurement. The magnitude of the dip depends on the IR laser power density, the population of the intermediate $v'=2$ level, and the Hönl–London factor for the overtone transition, the latter being stronger for R_1 lines than for P_1 lines and both increasing with N. The percentage depletion can approach 100% in these experiments, as OH radicals promoted to the $v=4$ state rapidly predissociate and are not cycled back to the intermediate $v'=2$ level. The magnitude of the depletions were kept at the 10%–20% level for linewidth measurements to minimize "depletion" broadening;[8] this was achieved by adjusting the IR laser power density. Increasing the percentage depletion from 10% to 20% did not result in a measurable broadening of the lines. Since the $[(\mathrm{UV}+\mathrm{IR})-\mathrm{UV}]$ signal level typically varies by ±2% due to pulsed laser fluctuations, even in the absence of an IR transition, dips of at least 10% in magnitude were needed to obtain adequate signal-to-noise ratios for accurate fitting of the line profiles.

IV. DISCUSSION

The FDIR measurements of the $4 \leftarrow 2$ vibrational overtone band in the excited OH $A\ ^2\Sigma^+$ electronic state were used to obtain spectroscopic constants for $v=4$. As shown in Table II, the rotational constants (B_4, D_4, and γ_4) obtained for $v=4$ are in good agreement with values from a merged fit by Coxon *et al.*,[32] which included data from two prior experimental studies of OH $A\ ^2\Sigma^+$ ($v=4$): LIF excitation spectroscopy on the $A\ ^2\Sigma^+ \leftarrow X\ ^2\Pi$ (4,2) transition[13] and dispersed fluorescence spectroscopy on the $B\ ^2\Sigma^+ \rightarrow A\ ^2\Sigma^+$ (1,4) transition.[14] The constants $G(4)$, ν_0 and B_4 are also in good accord with the values derived from Dunham coefficients,[33] which are based on a compilation of spectroscopic data for the OH $A\ ^2\Sigma^+$ state up to $v=9$. The line positions reported here can, in principle, be combined with earlier experimental data in a global fit to obtain refined values for the spectroscopic constants of the OH $A\ ^2\Sigma^+$ state. However, this is beyond the scope of the present work, which is focused primarily on predissociation dynamics.

Prior to the present experimental study, the predissociation lifetimes of the OH $A\ ^2\Sigma^+$ ($v=0-4, N$) levels had been investigated theoretically by Parlant and Yarkony[1] and Yarkony.[4] Their calculations were carried out using exact time-independent quantum dynamics based on spin-orbit and Coriolis couplings derived from multireference configuration-interaction wave functions. In addition, they performed approximate calculations based on the Fermi golden rule, which yielded very similar lifetimes. The predissociation rates were found to be largely determined by the spin-orbit interaction in the crossing region between the $A\ ^2\Sigma^+$ state and the repulsive curves ($^4\Sigma^-$, $^2\Sigma^-$, and $^4\Pi$). Thus, the location of a rovibrational level relative to a crossing determines the importance of a particular repulsive potential in inducing predissociation and the rate for this process.

The $A\ ^2\Sigma^+$ ($v=0-3$) levels at low N lie below the crossing with the lowest repulsive state ($^4\Sigma^-$), and predissociation of these levels is predicted to proceed through a single dissociative potential ($^4\Sigma^-$).[1,4] For the $v=0$ to 3 levels, there is a strong increase in the rate of predissociation with N, due to the increased spin-orbit coupling as the rovibrational level approaches the $^4\Sigma^-$ crossing. On the other hand, the $A\ ^2\Sigma^+$ ($v=4$) level at low N lies between the $^4\Sigma^-$ and $^2\Sigma^-$ crossings and, as a result, decays through spin-orbit interactions with multiple repulsive potentials ($^4\Sigma^-$, $^2\Sigma^-$, and $^4\Pi$).[1] Consequently, the predissociation lifetimes in $v=4$ are computed to be much shorter (by a factor of 10 or more) than those in $v=3$ of the $A\ ^2\Sigma^+$ state. For $A\ ^2\Sigma^+$ ($v=4, N=0$), predissociation is predominantly a result of interaction with the lowest repulsive $^4\Sigma^-$ potential ($\sim 72\%$), while for $N=14$ the highest repulsive $^4\Pi$ potential dominates ($\sim 78\%$).[1] Furthermore, the predissociation lifetimes for $v=4$ are predicted to be relatively invariant with N, decreasing from 19 to 13 ps for the F_1 levels with $N=0$ to 10. The F_2 levels are computed to have essentially the same lifetimes of the corresponding F_1 levels, and thus the experimental work focuses on the F_1 levels only. The weak N dependence appears to result from the unusual coupling of three different potentials to the $A\ ^2\Sigma^+$ ($v=4, N$) levels.

The experimental lifetimes, obtained directly from the linewidths of FDIR spectra (Fig. 3), vary between 23(5) and 17(3) ps for the $N=0$ to 7 levels (F_1) in the $A\ ^2\Sigma^+$ ($v=4$) state. The experimental linewidths are in very good agreement with the theoretical predictions described above, and both are displayed in Fig. 4. In addition, the experimental

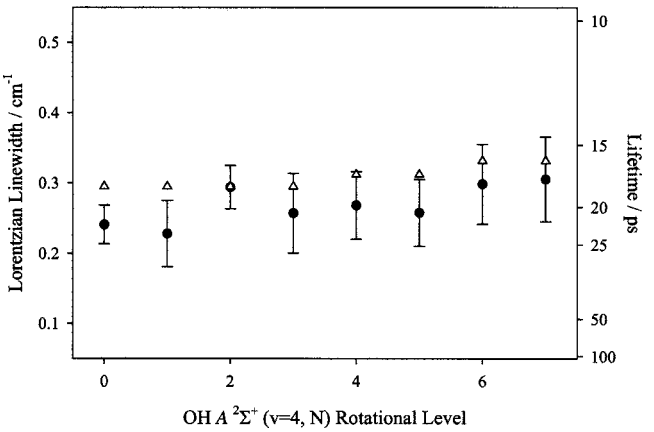

FIG. 4. Linewidths and corresponding lifetimes of OH $A\,^2\Sigma^+$ $(v=4,N)$ rotational levels derived from the Lorentzian component of FDIR line profiles (filled circles) and first-principles theory (open triangles; Ref. 1). The linewidths are nearly invariant over the range of rotational levels examined.

values are relatively unchanged with N, showing only a slightest trend of increasing linewidth with N, in accord with theoretical predictions.[1]

The present linewidth measurements are significantly different (by a factor of 3) than the experimental results of Copeland *et al.*,[13] in which linewidths of 0.65–1.0 cm^{-1} were reported for the OH $A\,^2\Sigma^+$ $(v=4,N=0-11)$ levels. The discrepancy most likely originates from the experimental linewidth of $\sim$0.6 cm^{-1} in the earlier measurements, which results from a convolution of the Doppler width at flame temperatures ($\sim$0.5 cm^{-1} near 2000 K) and the laser bandwidth.[13] Thus, the present experiments performed with a single-mode optical parametric oscillator (0.02-cm^{-1} bandwidth) under jet conditions yield improved linewidth measurements for the $N=0$ to 7 levels of the $A\,^2\Sigma^+$ $(v=4)$ state.

The lifetime of the intermediate $A\,^2\Sigma^+$ $(v'=2,N')$ state presents a limitation in the present FDIR measurements. The total lifetime of the $v'=2$ intermediate state decreases from 122 ns for $N'=0$ to 47 ns for $N'=7$,[11] as a result of the increase in the rate of predissociation with N'. There is a concomitant decrease in the fluorescence quantum yield with N', which drops from $\Phi_{fl}=0.151$ to 0.055 for $N'=0$ to 7.[11] A combination of the decrease in the fluorescence lifetime and reduction in fluorescence quantum yield for the intermediate state has precluded measurement of transition frequencies and/or linewidths for OH $A\,^2\Sigma^+$ $(v=4,N>7)$.

V. CONCLUSIONS

An UV-IR double-resonance technique has been employed to access highly predissociative rovibrational levels of the excited $A\,^2\Sigma^+$ electronic state of the OH radical. The UV excitation prepares a single rovibronic level of the $A\,^2\Sigma^+$ $(v'=2)$ state, and subsequent IR excitation is used to access the $A\,^2\Sigma^+$ $(v=4)$ state. Spectroscopic studies of the $4\leftarrow2$ overtone transition yield the vibrational origin as well as rotational, centrifugal distortion, and spin-rotation constants for the OH $A\,^2\Sigma^+$ $(v=4)$ state. The resultant values are in good accord with spectroscopic parameters for the OH $A\,^2\Sigma^+$ state derived from other types of measurements.[13,14,32] The predissociation dynamics of the OH $A\,^2\Sigma^+$ $(v=4)$ state is examined through linewidth measurements. The Lorentzian linewidths extracted from Voigt line profiles demonstrate that the $N=0$ to 7 rotational levels of the OH $A\,^2\Sigma^+$ $(v=4)$ state undergo rapid predissociation, with lifetimes on the order of 20 ps. The experimental lifetimes are in excellent accord with first-principles theoretical studies,[1,4] which have attributed the rapid decay to spin-orbit coupling with three repulsive potentials ($^4\Sigma^-$, $^2\Sigma^-$, and $^4\Pi$). The lifetimes indicate that the fluorescence quantum yield from the OH $A\,^2\Sigma^+$ $(v=4)$ state is essentially zero ($\sim10^{-5}$). In the present experiments, fluorescence is detected exclusively from the $A\,^2\Sigma^+$ $(v'=2)$ state, with a dip detected each time the IR laser is resonant with an overtone transition.

FDIR spectroscopy is useful for investigating systems in which the upper state is not easily detected due to a low-fluorescence quantum yield. Consequently, it has high utility for linewidth measurements of highly predissociative states, such as the OH $A\,^2\Sigma^+$ $(v=4)$ state reported here. The double-resonance aspect of the method may also make it advantageous in situations where a direct excitation process has poor Franck–Condon overlap. Future studies may include the investigation of higher vibrational levels of the $A\,^2\Sigma^+$ state of the hydroxyl radical and its deuterated analog. In addition, FDIR spectroscopy can be extended to polyatomic systems, e.g., alkoxy radicals,[34] which have low-fluorescence quantum yields in excited electronic states due to predissociation or other nonradiative decay processes.

ACKNOWLEDGMENTS

This research has been supported by the Air Force Office of Scientific Research under Contract No. FA9550-04-1-0068. Partial equipment support was provided by the National Science Foundation and the Department of Energy. The authors thank Mark D. Marshall (Amherst) for helpful advice and supplying the least-squares-fitting routine used in the rotational analysis, and Ian M. Konen for help with analysis of Voigt line profiles.

[1] G. Parlant and D. R. Yarkony, J. Chem. Phys. **110**, 363 (1999).
[2] C. Kalyanaraman and N. Sathyamurthy, Chem. Phys. **187**, 219 (1994).
[3] M. L. Sink, A. D. Bandrauk, and R. Lefebvre, J. Chem. Phys. **73**, 4451 (1980).
[4] D. R. Yarkony, J. Chem. Phys. **97**, 1838 (1992).
[5] K. R. German, J. Chem. Phys. **63**, 5252 (1975).
[6] K. R. German, J. Chem. Phys. **62**, 2584 (1975).
[7] J. Brzozowski, P. Erman, and M. Lyyra, Phys. Scr. **17**, 507 (1978).
[8] J. A. Gray and R. L. Farrow, J. Chem. Phys. **95**, 7054 (1991).
[9] D. E. Heard, D. R. Crosley, J. B. Jeffries, G. P. Smith, and A. Hirano, J. Chem. Phys. **96**, 4366 (1992).
[10] J. J. L. Spaanjaars, J. J. ter Meulen, and G. Meijer, J. Chem. Phys. **107**, 2242 (1997).
[11] J. Luque and D. R. Crosley, SRI International Report No. MP 99, 1999 (unpublished).
[12] W. Zhou, Y. Yuan, and J. Zhang, J. Chem. Phys. **119**, 9989 (2003).
[13] R. A. Copeland, J. B. Jeffries, and D. R. Crosley, J. Mol. Spectrosc. **143**, 183 (1990).
[14] C. Carlone and F. W. Dalby, Can. J. Phys. **47**, 1945 (1969).
[15] Wilmad Labglass, Suprasil 300, 0.5-mm i.d.$\times$5-mm o.d.$\times$10-mm length.
[16] G. H. Dieke and H. M. Crosswhite, J. Quant. Spectrosc. Radiat. Transf. **2**, 97 (1962).
[17] L. S. Rothman, C. P. Rinsland, A. Goldman *et al.*, J. Quant. Spectrosc. Radiat. Transf. **60**, 665 (1998).
[18] I. B. Pollack, M. Tsiouris, H. O. Leung, and M. I. Lester, J. Chem. Phys.

119, 118 (2003).
[19] Y. Kim, J. Fleniken, and H. Meyer, J. Chem. Phys. **114**, 5577 (2001).
[20] G. M. Florio, E. L. Sibert, III, and T. S. Zwier, Faraday Discuss. **118**, 315 (2001).
[21] G. Herzberg, *Molecular Spectra and Molecular Structure. I. Spectra of Diatomic Molecules* (Van Nostrand, New York, 1950).
[22] The OH $A\,^2\Sigma^+$ state is well described using Hund's case (b) notation with the quantum number for the total angular momentum labeled J and that for rotation (without spin) labeled N. The rotational levels are shifted slightly due to spin-rotation coupling (see text), with fine-structure labeling of $N=J-\frac{1}{2}$ for the F_1 spin component and $N=J+\frac{1}{2}$ for the F_2 spin component. Spectroscopic transitions use ΔN notation with subscripts denoting the spin component(s) of the upper state and, if different, the lower state, e.g., R_1 for a $\Delta N=+1$ transition involving the F_1 spin component.
[23] While no significant amount of vibrationally excited OH has been reported upon 193-nm photolysis of HNO_3 at modest laser fluences (<5 mJ/cm^2) (Refs. 24–27) some OH $X\,^2\Pi(v''=1,J'')$ is detected at the much higher laser fluence ($\sim$24 mJ/cm^2) used in the present study. We suspect that the production of vibrationally excited OH may be due to absorption of two or more 193-nm photons, e.g., $HNO_3 \rightarrow HONO+O \rightarrow OH\ A\,^2\Sigma^+ + NO + O$, followed by radiative decay (Refs. 28 and 29).
[24] Q. Li, R. T. Carter, and J. R. Huber, Chem. Phys. Lett. **334**, 39 (2001).
[25] G.-H. Leu, C.-W. Hwang, and I. C. Chen, Chem. Phys. Lett. **257**, 481 (1996).
[26] A. Schiffman, D. D. Nelson, Jr., and D. J. Nesbitt, J. Chem. Phys. **98**, 6935 (1993).
[27] A. Jacobs, K. Kleinermanns, H. Kuge, and J. Wolfrum, J. Chem. Phys. **79**, 3162 (1983).
[28] A. A. Turnipseed, G. L. Vaghjiani, J. E. Thompson, and A. R. Ravishankara, J. Chem. Phys. **96**, 5887 (1992).
[29] R. D. Kenner, F. Rohrer, and F. Stuhl, J. Phys. Chem. **90**, 2635 (1986).
[30] D. R. Guyer, L. Huwel, and S. R. Leone, J. Chem. Phys. **79**, 1259 (1983).
[31] J. A. Coxon, Can. J. Phys. **58**, 933 (1980).
[32] J. A. Coxon, A. D. Sappey, and R. A. Copeland, J. Mol. Spectrosc. **145**, 41 (1991).
[33] J. Luque and D. R. Crosley, J. Chem. Phys. **109**, 439 (1998).
[34] S. Gopalakrishnan, L. Zu, and T. A. Miller, Chem. Phys. Lett. **380**, 749 (2003).